Influence of single scattering and multiple scattering on backscattered Mueller matrix in turbid media

Lanqing Xu (徐兰青), Hui Li (李 晖)*, and Yongping Zheng (郑勇平)

Key Laboratory of Opto-Electronic Science and Technology for Medicine (Fujian Normal University), Ministry of Education, Fujian Provincial Key Lab of Photonic Technology, Fuzhou 350007

**E-mail: hli@fjnu.edu.cn*

Received September 2, 2008

Monte Carlo algorithm and Stokes-Mueller formalism are used to simulate the propagation behavior of polarized light in turbid media. The influence of single scattering and multiple scattering on backscattered Mueller matrix in turbid media is discussed. Single and double scattering photons form the major part of backscattered polarization patterns, while multiple scattering photons present more likely as background. Further quantitative analyses show that single scattering approximation and double scattering approximation are quite accurate when discussing the polarization patterns near the incident point.

OCIS codes: 170.5280, 260.5430, 290.1350, 290.7050.
doi: 10.3788/COL20090701.0064.

Recently, propagation of polarized light in turbid media such as bio-tissue has attracted significant interest because of its promising applications in noninvasive optical diagnosis and imaging. Several studies have demonstrated that relevant information of turbid media can be derived by analyzing the backscattered Mueller matrix patterns[1−9]. Many published works suggested that the main contribution to effective Mueller matrix came from those weakly scattered photons and used single scattering or double scattering approximations[6−9]. But the validity of these approximations was seldom discussed before. In this letter, the backscattered Mueller matrix is calculated using Monte Carlo (MC) algorithm[10,11] and Stokes-Mueller formalism. Moreover, the influence of scattering events on backscattered polarization patterns is analyzed quantitatively by the use of user-defined functions.

We assume that light is scattered by spheres and Mie theory can be applied. The MC method is implemented under the following assumptions: elastic scattering, steady state, independent scattering events, and no coherent effects. Changes in polarization when photons are scattered are conducted in the far-field approximation. The incoming narrow beam of incoherent light propagates downwards along z axis into a semi-infinite slab containing randomly distributed homogeneous particles, as shown in Fig. 1. Let $\mathbf{S}_i$ be the Stokes vector of incident beam with respect to the laboratory coordinate system (x, y, z). Using the Stokes-Mueller formalism, the Stokes vectors $\mathbf{S}_{\rm bs}^n$ of a backscattered photon packet after n scattering could be

$$\begin{aligned}\mathbf{S}_{\rm bs}^n &= [\mu_{\rm s}/(\mu_{\rm a}+\mu_{\rm s})]^n R(\phi_t) M_t M(\theta_n) R(\phi_n) \cdots \\ &\quad M(\theta_2) R(\phi_2) M(\theta_1) R(\phi_1) \mathbf{S}_i \\ &= [\mu_{\rm s}/(\mu_{\rm a}+\mu_{\rm s})]^n M^n \mathbf{S}_i, \end{aligned} \tag{1}$$

where $\mu_{\rm s}$ and $\mu_{\rm a}$ are the scattering and absorption coefficients respectively, $M(\theta)$ is the scattering matrix derived from Mie theory[12], $R(\phi)$ is the rotation matrix connecting the Stokes vectors of reference plane and scattering plane, $R(\phi_t)$ transforms the Stokes vector of light in the local coordinate system back to the laboratory coordinate system before the photon packet is received by the detector, M_t is the Fresnel matrix that describes the refraction at the surface[9], M^n is believed to be the sample's effective backscattered Mueller matrix of n scattering after further normalization.

The 16 elements of Mueller matrix denote different polarized properties of turbid media. For conciseness, here we discuss only 4 matrix elements, which are M_{11}, M_{12}, M_{13}, and M_{22}. To analyze the backscattered Mueller matrix of different numbers of scattering events quantitatively, we firstly integrate the two-dimensional (2D) distribution of Mueller matrix elements over radial axis r:

$$M_{ij}^n(\phi) = \frac{1}{r_{\max}} \int_0^{r_{\max}} M_{ij}^n(r,\phi) {\rm d}r. \tag{2}$$

Secondly, we integrate $M_{ij}^n(\phi)$ over azimuth direction and get

$$I_{ij}^n = \int_0^{\pi/4} M_{ij}^n(\phi) {\rm d}\phi. \tag{3}$$

Finally, we divide I_{ij}^n by $I_{ij}^{\rm total}$ and get the weight of each

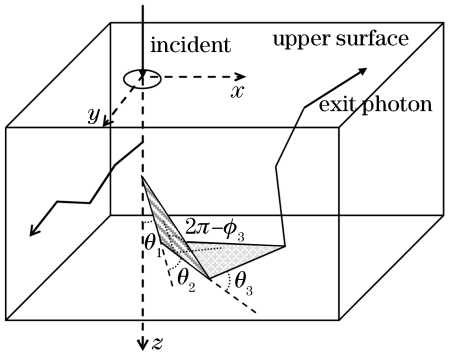

Fig. 1. Geometry of multiple scattering.

scattering matrix element in the total effective Mueller matrix element:

$$W_{ij}(n) = I_{ij}^{n}/I_{ij}^{\text{total}} \times 100\%. \quad (4)$$

In the following calculation, M_{ij}^{n} is derived only from those backscattered photons which encounter the nth scattering events in the media. Total backscattered Mueller matrix M_{ij}^{total} is calculated from all backscattered photons. Multiply scattered backscattered Mueller matrix M_{ij}^{mul} is calculated from all backscattered photons with scattering events greater than 20 times.

Based on Eq. (1), Mueller matrix patterns for light backscattered from turbid media are calculated. The incident light wavelength is 597 nm, and the sphere diameter is set as 97 nm. The refractive indices of scatters and media are 1.57 and 1.33, respectively[12,13]. The optical parameters are $\mu_a = 0.01\ \text{cm}^{-1}$, $\mu_s = 1.00\ \text{cm}^{-1}$, and the recording area size is 10×10 (cm).

Figure 2 demonstrates the 2D distribution of backscattered photons for different numbers of scattering events.

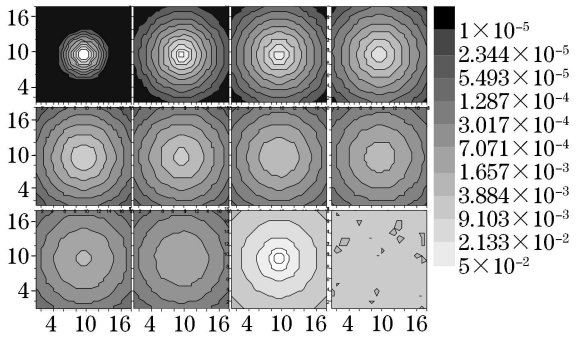

Fig. 2. 2D distribution of backscattered photon numbers for different numbers of scattering events. From upper to lower, from left to right, the first ten graphs stand in turn for scattering events from once to tenth. The eleventh and twelfth graphs are the distribution of total backscattered photons and multiply scattered photons (great than 20 times).

The profiles show clearly that weakly scattered photons exit more often from near the incident point and the quantity decreases quickly as the radius increases. Multiply scattered photons exit more likely from the outer area. More scattering events are, evener the distribution profile is.

Figure 3 shows M_{11}, M_{12}, M_{13}, and M_{22} matrix elements for different numbers of scattering events. It can be seen from this figure that the features of single scattering matrix can be well preserved in the diffusely backscattered Mueller matrix M_{ij}^{total}. As the number of scattering events increases, the matrix patterns become blurred. For multiply scattered backscattered Mueller matrix M_{ij}^{mul}, only randomly distributed signals can be seen and the matrix patterns disappear totally.

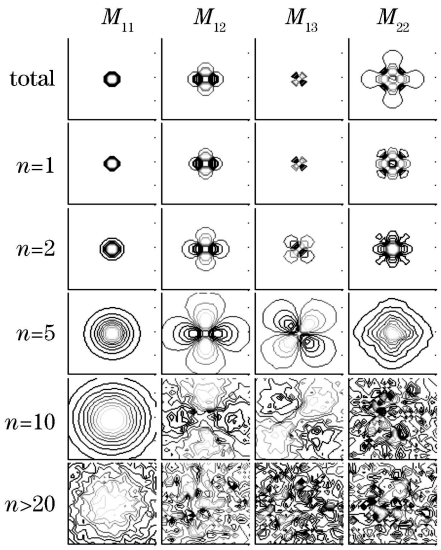

Fig. 3. M_{11}, M_{12}, M_{13}, and M_{22} elements for different numbers of scattering events. n stands for number of scattering events that the recorded photons encounter in the medium.

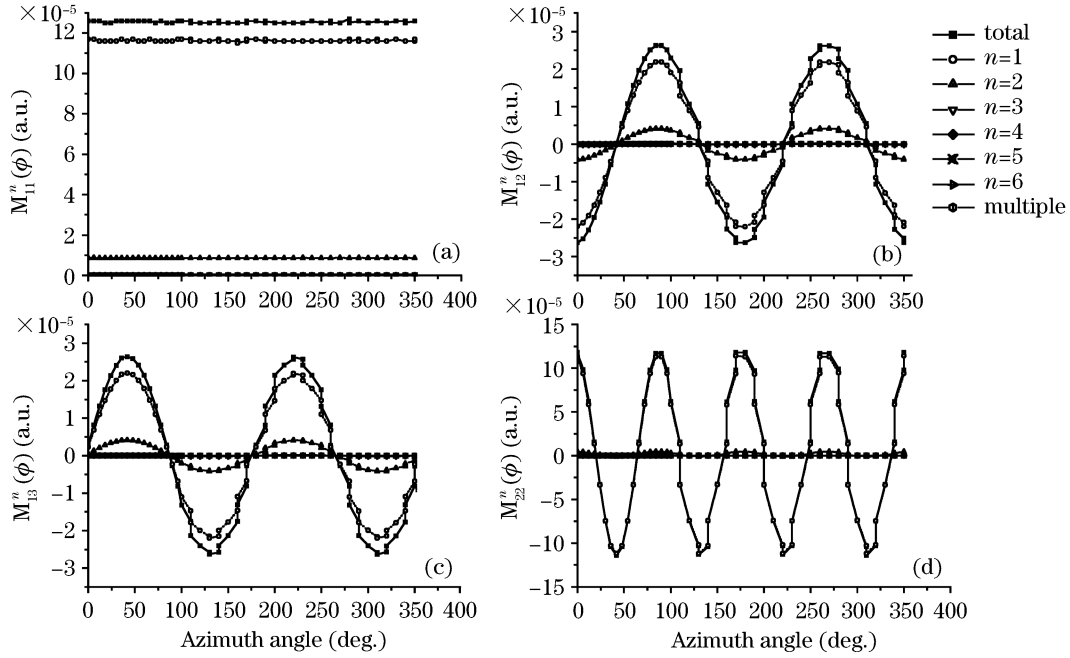

Fig. 4. (a) $M_{11}^{n}(\phi)$, (b) $M_{12}^{n}(\phi)$, (c) $M_{13}^{n}(\phi)$, (d) $M_{22}^{n}(\phi)$ calculated from M_{11}, M_{12}, M_{13}, M_{22} elements for different numbers of scattering events.

Table 1. Weights of Mueller Matrix Elements W_{ij} of Different Numbers of Scattering Events n in the Total Effective Mueller Matrix Elements (%)

n	1	2	3	4	5	6	> 20
W_{11}	92.7	6.8	0.4	0.0	0.0	0.0	0.0
W_{12}	83.4	15.8	0.8	0.0	0.0	0.0	0.0
W_{13}	83.4	15.7	0.8	0.0	0.0	0.0	0.0
W_{22}	95.1	4.7	0.2	0.0	0.0	0.0	0.0

To compare each M_{ij}^n numerically, we use Eq. (2) to calculate $M_{ij}^{\text{total}}(\phi)$, $M_{ij}^{\text{mul}}(\phi)$, and $M_{ij}^n(\phi)$ for n varied from one to six and get Fig. 4. It is seen that single scattering matrix takes the major part of total matrix, double scattering comes next, and other portion only forms a tiny part. To analyze the contribution of each M_{ij}^n to M_{ij}^{total} quantitatively, we further apply Eqs. (3) and (4) to Fig. 4 and get the data listed in Table 1. It is indicated that single scattering and double scattering totally weight more than 99% in the total backscattered Mueller matrix, and single scattering portion takes up the major part. That means single scattering feature can be well preserved in total effective Mueller matrix. For backscattered photons with scattering events more than 3 times, they totally contribute less than 1% to total backscattered Mueller matrix. As their distributions are rather even compared to single and double scattering photons, they will represent as background in the total backscattered Mueller matrix.

Using Monte Carlo method and Stokes-Mueller formalism, we calculated the backscattered Mueller matrix for M_{11}, M_{12}, M_{13} and M_{22} elements of different numbers of scattering events. Results show that single and double scattering photons exit from near the incident point and form the major part of backscattered polarization patterns. In the area of 10 mean free paths (mfp) around incident point, their contribution to the total matrix amounts to more than 99%. Multiply scattered photons exit from the outer area and present more likely as background in the total backscattered Mueller matrix. These conclusions firmly proved that single scattering and double scattering approximations are quite accurate when discussing the polarization patterns near the incident point.

This work was supported in part by the National Natural Science Foundation of China (No. 60578056) and in part by the Natural Science Foundation of Fujian Province of China (No. A0520001).

References

1. J. Dillet, C. Baravian, F. Caton, and A. Parker, Appl. Opt. **45,** 4669 (2006).
2. D. Côté and I. A. Vitkin, Opt. Express **13,** 148 (2005).
3. M. Xu, Opt. Express **12,** 6530 (2004).
4. M. J. Raković, G. W. Kattawar, M. Mehrűbeoğlu, B. D. Cameron, L. V. Wang, S. Rastegar, and G. L. Coté, Appl. Opt. **38,** 3399 (1999).
5. Y. Li, R. Chen, H. Zeng, Z. Huang, S. Feng, and S. Xie, Chin. Opt. Lett. **5,** 105 (2007).
6. S. Bartel and A. H. Hielscher, Appl. Opt. **39,** 1580 (2000).
7. M. J. Raković and G. W. Kattawar, Appl. Opt. **37,** 3333 (1998).
8. X. Wang, G. Yao, and L. V. Wang, Appl. Opt. **41,** 792 (2002).
9. L. Xu, H. Li, and S. Xie, Acta Phys. Sin. (in Chinese) **57,** 6024 (2008).
10. L. Wang, S. L. Jacques, and L. Zheng, Comput. Methods Programs Biomed. **47,** 131 (1995).
11. J. C. Ramella-Roman, S. A. Prahl, and S. L. Jacques, Opt. Express **13,** 4420 (2005).
12. C. F. Bohren and D. R. Huffman, *Absorption and Scattering of Light by Small Particles* (John Wiley, New York, 1983).
13. L. Xu, H. Li, and S. Xie, Chin. Opt. Lett. **5,** 102 (2007).